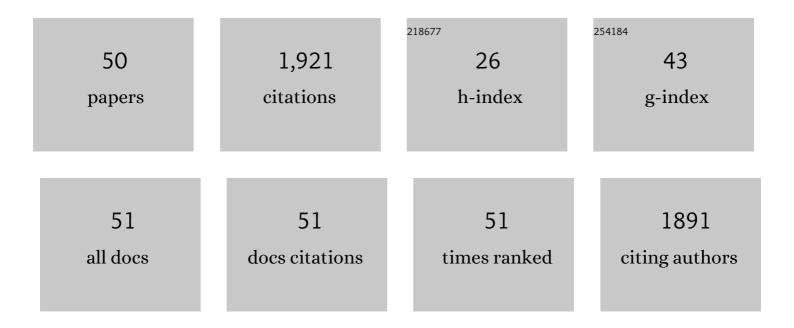
## Hongye Bai

List of Publications by Year in descending order

Source: https://exaly.com/author-pdf/1338977/publications.pdf Version: 2024-02-01



#	Article	IF	CITATIONS
1	Self-templated transformation of MOFs into layered double hydroxide nanoarrays with selectively formed Co9S8 for high-performance asymmetric supercapacitors. Chemical Engineering Journal, 2018, 354, 716-726.	12.7	179
2	In-situ approach to fabricate BiOI photocathode with oxygen vacancies: Understanding the N2 reduced behavior in photoelectrochemical system. Chemical Engineering Journal, 2019, 362, 349-356.	12.7	121
3	Efficient Electrocatalytic Oxidation of 5-Hydroxymethylfurfural Coupled with 4-Nitrophenol Hydrogenation in a Water System. ACS Catalysis, 2022, 12, 1545-1557.	11.2	113
4	In-situ implantation of plasmonic Ag into metal-organic frameworks for constructing efficient Ag/NH2-MIL-125/TiO2 photoanode. Chemical Engineering Journal, 2020, 388, 124206.	12.7	98
5	An in situ photoelectroreduction approach to fabricate Bi/BiOCl heterostructure photocathodes: understanding the role of Bi metal for solar water splitting. Journal of Materials Chemistry A, 2017, 5, 4894-4903.	10.3	96
6	In-situ anchoring Ag through organic polymer for configuring efficient plasmonic BiVO4 photoanode. Chemical Engineering Journal, 2019, 358, 658-665.	12.7	81
7	MOF-derived Co3O4 thin film decorated BiVO4 for enhancement of photoelectrochemical water splitting. Applied Surface Science, 2019, 491, 497-504.	6.1	77
8	Organic-inorganic hybrid-photoanode built from NiFe-MOF and TiO2 for efficient PEC water splitting. Electrochimica Acta, 2020, 349, 136383.	5.2	72
9	Core-shell structured ZnCo2O4@ZnWO4 nanowire arrays on nickel foam for advanced asymmetric supercapacitors. Journal of Colloid and Interface Science, 2018, 531, 64-73.	9.4	71
10	Fabrication of MgFe <sub>2</sub> O <sub>4</sub> /MoS <sub>2</sub> Heterostructure Nanowires for Photoelectrochemical Catalysis. Langmuir, 2016, 32, 1629-1636.	3.5	59
11	Semiconductors with NIR driven upconversion performance for photocatalysis and photoelectrochemical water splitting. CrystEngComm, 2014, 16, 3059.	2.6	54
12	Fabrication of BiVO4-Ni/Co3O4 photoanode for enhanced photoelectrochemical water splitting. Applied Surface Science, 2021, 538, 148150.	6.1	51
13	Understanding the key role of vanadium in p-type BiVO4 for photoelectrochemical N2 fixation. Chemical Engineering Journal, 2021, 414, 128773.	12.7	50
14	Heterojunction composites of g-C3N4/KNbO3 enhanced photocatalytic properties for water splitting. International Journal of Hydrogen Energy, 2018, 43, 16566-16572.	7.1	46
15	Fabrication of Au@CdS/RGO/TiO <sub>2</sub> heterostructure for photoelectrochemical hydrogen production. New Journal of Chemistry, 2016, 40, 2287-2295.	2.8	36
16	Boosting Water Splitting Performance of BiVO <sub>4</sub> Photoanode through Selective Surface Decoration of Ag <sub>2</sub> S. ChemCatChem, 2018, 10, 4927-4933.	3.7	35
17	Amorphous MnCO <sub>3</sub> /C Double Layers Decorated on BiVO <sub>4</sub> Photoelectrodes to Boost Nitrogen Reduction. ACS Applied Materials & Interfaces, 2020, 12, 52763-52770.	8.0	35
18	Ag-Pi/BiVO4 heterojunction with efficient interface carrier transport for photoelectrochemical water splitting. Journal of Colloid and Interface Science, 2020, 579, 619-627.	9.4	35

Hongye Bai

#	Article	IF	CITATIONS
19	Understanding the Z-scheme heterojunction of BiVO <sub>4</sub> /PANI for photoelectrochemical nitrogen reduction. Chemical Communications, 2021, 57, 10568-10571.	4.1	35
20	Biothiol-Functionalized Cuprous Oxide Sensor for Dual-Mode Sensitive Hg <sup>2+</sup> Detection. ACS Applied Materials & Interfaces, 2021, 13, 46980-46989.	8.0	34
21	Reasonable regulation of kinetics over BiVO4 photoanode by Fe–CoP catalysts for boosting photoelectrochemical water splitting. International Journal of Hydrogen Energy, 2019, 44, 28184-28193.	7.1	33
22	Charge-transfer dynamics at a Ag/Ni-MOF/Cu <sub>2</sub> 0 heterostructure in photoelectrochemical NH <sub>3</sub> production. Chemical Communications, 2021, 57, 8031-8034.	4.1	33
23	In-situ decoration of unsaturated Cu sites on Cu2O photocathode for boosting nitrogen reduction reaction. Chemical Engineering Journal, 2021, 413, 127453.	12.7	31
24	Integrated Heterostructure of PDA/Biâ€AgIn <sub>5</sub> S <sub>8</sub> /TiO <sub>2</sub> for Photoelectrochemical Hydrogen Production: Understanding the Synergistic Effect of Multilayer Structure. Advanced Materials Interfaces, 2018, 5, 1701574.	3.7	29
25	Fabrication of Zn-MOF decorated BiVO4 photoanode for water splitting. Colloids and Surfaces A: Physicochemical and Engineering Aspects, 2022, 640, 128412.	4.7	29
26	Synthesis of C/Co <sub>3</sub> O <sub>4</sub> composite mesoporous hollow sphere sandwich graphene films for high-performance supercapacitors. Inorganic Chemistry Frontiers, 2018, 5, 2554-2562.	6.0	26
27	Photoelectrochemical detection of 4-nitrophenol by sensitive Ni/Cu2O photocathode. Electrochimica Acta, 2021, 367, 137453.	5.2	26
28	Rod-in-tube nanostructure of MgFe <sub>2</sub> O <sub>4</sub> : electrospinning synthesis and photocatalytic activities of tetracycline. New Journal of Chemistry, 2016, 40, 538-544.	2.8	25
29	Hydrothermal synthesis of <font>Fe</font> <sub>2</sub> <font>O</font> <sub>3</sub> / <font>ZnO</font> heterojunction photoanode for photoelectrochemical water splitting. Functional Materials Letters, 2015, 08, 1550058.	1.2	24
30	Hierarchical CoP@Ni <sub>2</sub> P core–shell nanosheets for ultrahigh energy density asymmetric supercapacitors. Inorganic Chemistry Frontiers, 2020, 7, 3030-3038.	6.0	24
31	Dual-functional electrochemical bio-sensor built from Cu2O for sensitively detecting the thiols and Hg2+. Applied Surface Science, 2021, 564, 150397.	6.1	22
32	Effect of unsaturated coordination on photoelectrochemical properties of Ni-MOF/TiO2 photoanode for water splitting. International Journal of Hydrogen Energy, 2021, 46, 17741-17750.	7.1	21
33	Photoelectrochemical reduction of nitrate to ammonia over CuPc/CeO2 heterostructure: Understanding the synergistic effect between oxygen vacancies and Ce sites. Chemical Engineering Journal, 2022, 433, 133225.	12.7	21
34	In Situ Electrochemical Reconstitution of CF–CuO/CeO <sub>2</sub> for Efficient Active Species Generation. Inorganic Chemistry, 2022, 61, 8940-8954.	4.0	21
35	In Situ Decorating Coordinatively Unsaturated Fe Sites for Boosting Water Oxidation Performance of TiO 2 Photoanode. Energy Technology, 2019, 7, 1801128.	3.8	20
36	Boosted Photoelectrochemical N <sub>2</sub> Reduction over Mo <sub>2</sub> C In Situ Coated with Graphitized Carbon. Langmuir, 2020, 36, 14802-14810.	3.5	20

Hongye Bai

#	Article	IF	CITATIONS
37	Sandwichâ€Nanostructured NiO–ZnO Nanowires@αâ€Fe <sub>2</sub> O <sub>3</sub> Film Photoanode with a Synergistic Effect and p–n Junction for Efficient Photoelectrochemical Water Splitting. ChemElectroChem, 2014, 1, 2089-2097.	3.4	19
38	Synthesis and Photoelectrochemical Properties of Efficient Photoanodes Built from Fe <sub>2</sub> O <sub>3</sub> /NiO Heterostructures. European Journal of Inorganic Chemistry, 2014, 2014, 3608-3613.	2.0	12
39	Ni-MOF <i>in-situ</i> Decorating ZnO photoelectrode for photoelectrochemical water splitting. Functional Materials Letters, 2018, 11, 1850085.	1.2	12
40	Fabrication of an amorphous metal oxide/p-BiVO <sub>4</sub> photocathode: understanding the role of entropy for reducing nitrate to ammonia. Inorganic Chemistry Frontiers, 2022, 9, 805-813.	6.0	12
41	Electrocatalytic reduction of 4-nitrophenol over Ni-MOF/NF: understanding the self-enrichment effect of H-bonds. Chemical Communications, 2022, 58, 4897-4900.	4.1	11
42	Hydrothermal synthesis of 3D Ba <sub>5</sub> Ta <sub>4</sub> O <sub>15</sub> flower-like microsphere photocatalytic properties. Journal of Materials Research, 2016, 31, 2640-2648.	2.6	10
43	Promoting photoelectrochemical hydrogen production performance by fabrication of Co1-XS decorating BiVO4 photoanode. International Journal of Hydrogen Energy, 2022, 47, 940-949.	7.1	10
44	An in-situ cation exchange approach to stabilize Zn-MOF: Understanding the role of nickel ions for photoelectrochemical performance. International Journal of Hydrogen Energy, 2022, 47, 10277-10288.	7.1	10
45	Confined growth of Co–Pi co-catalyst by organic semiconductor polymer for boosting the photoelectrochemical performance of BiVO <sub>4</sub> . New Journal of Chemistry, 2019, 43, 8160-8167.	2.8	9
46	An effective route for growth of WO3/BiVO4 heterojunction thin films with enhanced photoelectrochemical performance. Journal of Industrial and Engineering Chemistry, 2021, 104, 146-154.	5.8	9
47	Controllable TiO2 heterostructure with carbon hybrid materials for enhanced photoelectrochemical performance. New Journal of Chemistry, 2017, 41, 3460-3465.	2.8	8
48	One-step syntheses of MoS2/graphitic carbon composites with enhanced photocatalytic activity under visible light irradiation. New Journal of Chemistry, 2017, 41, 14171-14178.	2.8	8
49	Fabrication of stable photoanode built from ZnO nanosheets in situ decorated with carbon film. Functional Materials Letters, 2017, 10, 1750068.	1.2	4
50	HYDROTHERMAL SYNTHESIS, CRYSTAL STRUCTURE AND ELECTROCHEMICAL BEHAVIOR OF 2D HYBRID COORDINATION POLYMER. Functional Materials Letters, 2013, 06, 1350027.	1.2	3